

Coexistence Mechanism Between eMBB and uRLLC in 5G Wireless Networks

Anupam Kumar Bairagi¹, *Member, IEEE*, Md. Shirajum Munir², *Graduate Student Member, IEEE*,
 Madyan Alsenwi³, Nguyen H. Tran⁴, *Senior Member, IEEE*, Sultan S. Alshamrani⁵,
 Mehedi Masud⁶, *Senior Member, IEEE*, Zhu Han⁷, *Fellow, IEEE*,
 and Choong Seon Hong⁸, *Senior Member, IEEE*

Abstract—Ultra-reliable low-latency communication (*uRLLC*) and enhanced mobile broadband (*eMBB*) are two influential services of the emerging 5G cellular network. Latency and reliability are major concerns for *uRLLC* applications, whereas *eMBB* services claim for the maximum data rates. Owing to the trade-off among latency, reliability and spectral efficiency, sharing of radio resources between *eMBB* and *uRLLC* services, heads to a challenging scheduling dilemma. In this paper, we study the co-scheduling problem of *eMBB* and *uRLLC* traffic based upon the puncturing technique. Precisely, we formulate an optimization problem aiming to maximize the minimum expected achieved rate (*MEAR*) of *eMBB* user equipment (UE) while fulfilling the provisions of the *uRLLC* traffic. We decompose the original problem into two sub-problems, namely scheduling problem of *eMBB* UEs and *uRLLC* UEs while prevailing objective unchanged. Radio resources are scheduled among the *eMBB* UEs on a time slot basis, whereas it is handled for *uRLLC* UEs on a mini-slot basis. Moreover, for resolving the scheduling issue of *eMBB* UEs, we use penalty successive upper bound minimization (*PSUM*) based algorithm, whereas the optimal transportation model (*TM*) is adopted for solving the same problem of *uRLLC* UEs. Furthermore, a heuristic algorithm is also provided to solve the

first sub-problem with lower complexity. Finally, the significance of the proposed approach over other baseline approaches is established through numerical analysis in terms of the *MEAR* and fairness scores of the *eMBB* UEs.

Index Terms—Ultra-reliable low latency communications (*uRLLC*), enhanced mobile broadband (*eMBB*), coexistence, penalty successive upper bound minimization (*PSUM*), transportation model (*TM*), resource scheduling.

I. INTRODUCTION

THE wireless industries are going through different kinds of emerging applications and services along with the explosive trends of mobile traffic [1]. High-resolution video streaming, virtual reality (VR), augmented reality (AR), autonomous cars, smart cities and factories, artificial intelligence (AI) based services are some of these categories. It is foreseen that the mobile application market will flourish in a cumulative average growth rate (CAGR) of 29.1% during 2015 – 2020 [2]. Energy efficiency, latency, reliability, data rate, etc are distinct for separate applications and services. To handle these diversified requirements, International Telecommunication Union (ITU) has already classified 5G services into Ultra-reliable low-latency communication (*uRLLC*), massive machine-type communication (*mMTC*), and enhanced mobile broadband (*eMBB*) categories [3]. Gigabit per second (Gbps) level data rates are required for *eMBB* users, whereas connection density and energy efficiency are the major concern for *mMTC*, and *uRLLC* traffic focuses on extremely high reliability (99.999%) and remarkably low latency (0.25 ~ 0.30 ms/packet) [4].

Generally, the lions' share of wireless traffic is produced by *eMBB* UEs. *uRLLC* traffic is naturally infrequent and needs to be addressed spontaneously. The easiest way to settle this matter is to reserve some resources for *uRLLC*. However, under-utilization of radio resources may emerge from this approach, and generally, effective multiplexing of traffics is required. For efficient multiplexing of *eMBB* and *uRLLC* traffics, 3GPP has recommended a superposition/puncturing skeleton [4] and the short-TTI/puncturing approaches [5] in 5G cellular systems. Though the short-TTI mechanism is straightforward for implementation, it degrades spectral efficiency because of the massive overhead in the control channel. On the contrary, the puncturing strategy decreases the above overhead, although it necessitates an adequate mechanism for

Manuscript received February 4, 2020; revised June 18, 2020 and November 5, 2020; accepted November 14, 2020. Date of publication November 24, 2020; date of current version March 17, 2021. This work was partially supported by the National Research Foundation of Korea (NRF) grant funded by the Korea government (MSIT) (No. 2020R1A4A1018607) and by the MSIT(Ministry of Science and ICT), Korea, under the Grand Information Technology Research Center support program(IITP-2020-2015-0-00742) supervised by the IITP(Institute for Information & communications Technology Planning & Evaluation). The associate editor coordinating the review of this article and approving it for publication was D. Marabissi. (Corresponding author: Choong Seon Hong.)

Anupam Kumar Bairagi is with the Discipline of Computer Science and Engineering, Khulna University, Khulna 9208, Bangladesh, and also with the Department of Computer Science and Engineering, Kyung Hee University, Seoul 446-701, South Korea (e-mail: anupam@ku.ac.bd).

Md. Shirajum Munir, Madyan Alsenwi, and Choong Seon Hong are with the Department of Computer Science and Engineering, Kyung Hee University, Seoul 446-701, South Korea (e-mail: munir@khu.ac.kr; malsenwi@khu.ac.kr; cshong@khu.ac.kr).

Nguyen H. Tran is with the School of Computer Science, The University of Sydney, Sydney, NSW 2006, Australia (e-mail: nguyen.tran@sydney.edu.au).

Sultan S. Alshamrani is with the Department of Information Technology, Taif University, Taif 21944, Saudi Arabia (e-mail: susamash@tu.edu.sa).

Mehedi Masud is with the Department of Computer Science, College of Computers and Information Technology, Taif University, Taif 21944, Saudi Arabia (e-mail: mmasud@tu.edu.sa).

Zhu Han is with the Department of Electrical and Computer Engineering, University of Houston, Houston, TX 77004 USA, and also with the Department of Computer Science and Engineering, Kyung Hee University, Seoul 446-701, South Korea (e-mail: zhan2@uh.edu).

Color versions of one or more figures in this article are available at <https://doi.org/10.1109/TCOMM.2020.3040307>.

Digital Object Identifier 10.1109/TCOMM.2020.3040307

recognizing and healing the punctured case. Slot (1 ms) and mini-slot (0.125 ms) are proposed as time units for meeting the latency requirement of *uRLLC* traffic in the 5G new radio (NR). At the outset of a slot, *eMBB* traffic is scheduled and continues unchanged throughout the slot. If the same physical resources are used, *uRLLC* traffic is overridden upon the scheduled *eMBB* transmission.

Currently, much attention has been paid to resource sharing for offering quality-of-service(QoS) or quality-of-experience (QoE) to the users. Studies [6] and [7] investigate the sharing of an unlicensed spectrum between LTE and WiFi networks, however, the study [8] consider LTE-A and NB-IoT services for sharing the same resources. Study [9] solves user association and resource allocation problems. The study [9] consider the downlink of fog network to support QoS provisions of the *uRLLC* and *eMBB*. Some other studies, however, investigates and/or analyzes the influence of *uRLLC* traffic on *eMBB* [10]–[15] or presents architecture and/or framework for co-scheduling of *eMBB* and *uRLLC* traffic [16]–[19]. Moreover, some authors consider *eMBB* and *uRLLC* traffic in their coexisting/multiplexing proposals [20]–[27] where they apply puncturing technique.

As per our knowledge, concrete mathematical models and solutions, however, are lacking in most of these coexistence mechanisms. Most of the studies mainly focus on analysis, system-level design or framework. Thus, efficient coexistence proposals between *eMBB* and *uRLLC* traffic are needed in the literature. So, to enable *eMBB* and *uRLLC* services in 5G wireless networks, we propose an effective coexistence mechanism in this paper. Our preliminary work has been published in [23] where we have used a one-sided matching and heuristic algorithm, respectively, for resolving resource allocation problems of *eMBB* and *uRLLC* users. The major difference between [23] and current work is the involvement of penalty successive upper bound minimization (*PSUM*) and transportation model (*TM*) for solving similar problems. This paper mainly focuses on the followings:

- First, we formulate an optimization problem for *eMBB* UEs with some constraints, where the objective is to maximize the minimum expected rate of *eMBB* UEs over time.
- Second, to solve the optimization problem effectively, we decompose it into two sub-problems: resource scheduling for *eMBB* UEs, and resource scheduling of *uRLLC* UEs. *PSUM* is used to solve the first sub-problem, whereas the *TM* is employed to solve the second one.
- Third, we redefine the first sub-problem into a minimization problem for each slot and provide an algorithm based upon *PSUM* to obtain near-optimal solutions.
- Fourth, we redefine the second sub-problem as a minimization problem for each mini-slot within every slot and present the algorithm based upon minimum cell cost (*MCC*) and modified distribution (*MODI*) methods of the transportation model to find an optimal solution of the second sub-problem.
- Fifth, we also present a cost-effective heuristic algorithm for resolving the first sub-problem.

- Finally, we perform a comprehensive experimental analysis for the proposed scheduling approach and compare the results, minimum expected achieved rate (*MEAR*) and fairness [43] of the *eMBB* UEs, with the punctured scheduler (PS) [21], multi-user preemptive scheduler (MUPS) [25], random scheduler (RS), equally distributed scheduler (EDS), and matching based scheduler (MBS) approaches.

The remainder of the paper is systematized as follows. In Section II, we present the literature review. We explain the system model and present the problem formulation in Section III. The proposed solution approach of the above-mentioned problem is addressed in Section IV. In Section V, we provide experimental investigation, discussion, and comparison concerning the proposed solution. Finally, we conclude the paper in Section VI. A list of acronyms is provided in Table I.

II. LITERATURE REVIEW

Recently, both industry and academia focus on the study of multiplexing between *eMBB* traffic and *uRLLC* traffic on the same physical resources. Information-theoretic arguments-based performance analysis for *eMBB* and *uRLLC* traffic has performed in [10]. The authors consider both orthogonal multiple access (OMA) and non-orthogonal multiple access (NOMA) for uplink in cloud radio access network (C-RAN) framework. An insight into the performance trade-offs among the *eMBB* and *uRLLC* traffic is explained in [10]. In [11], authors have introduced *eMBB* influenced minimization problem to protect the *uRLLC* traffic from the dominant *eMBB* services. This paper explores their proposal for the mobile front-haul environment. In [12], the authors present an effective solution for multiplexing different traffics on a shared resource. Particularly, they propose an effective radio resource distribution method between the *uRLLC* and *eMBB* service classes following trade-offs among the reliability, latency and spectral efficiency. Moreover, they investigate the *uRLLC* and *eMBB* performance adopting different conditions.

In order to achieve 5G service provisioning (i.e., *eMBB*, mMTC and *uRLLC* services), the authors of [13] have studied radio resources slicing mechanism, where the performance of both orthogonal and non-orthogonal are analyzed. They have proposed a communication-theoretic model by considering the heterogeneity of 5G services. They also found that the non-orthogonal slicing is significantly better to perform instead of orthogonal slicing for those 5G service multiplexing. Recently, for 5G NR physical layer challenges and solution mechanisms of *uRLLC* traffic communications has been presented in [14], where they pay attention to the structure of packet and frame. Additionally, they focus on the improvement of scheduling and reliability mechanism for *uRLLC* traffic communication such that the coexistence of *uRLLC* with *eMBB* is established. In [15], the authors have been analyzed the designing principle of the 5G wireless network by employing low-latency and high-reliability for *uRLLC* traffic. To do this, they consider varying requirements of *uRLLC* services such as variation of delay, packet size, and reliability. To an extent, they explore different topology network architecture under the uncertainty.

TABLE I
LIST OF ABBREVIATIONS

Abbreviation	Elaboration
uRLLC	Ultra-reliable Low-latency Communication
eMBB, MBB	Enhanced Mobile Broadband, Mobile Broadband
mMTC	Massive Machine-type Communication
PSUM, SUM	Penalty Successive Upper bound Minimization, Successive Upper bound Minimization
TTI	Transmission Time Interval
NR	New Radio
QoS	Quality-of-Service
QoE	Quality-of-Experience
TM, BTM	Transportation Model, Balanced Transportation Model
MCC	Minimum Cell Cost
MODI	Modified Distribution
PS	Punctured Scheduler
MUPS	Multi-User Preemptive Scheduler
RS	Random Scheduler
EDS	Equally Distributed Scheduler
MBS	Matching Based Scheduler
MEAR	Minimum Expected Achieved Rate
NOMA, OMA	Non-orthogonal Multiple Access, Orthogonal Multiple Access
PRB, RB	Physical Resource Block, Resource Block
MIMO	Multiple-input Multiple-output
SINR	signal-to-interference-noise-ratio
gNB	Next Generation Base Station
CP	Combinatorial Programming
CDF, ECDF	Cumulative Distribution Function, Empirical Cumulative Distribution Function
NWC	Northwest corner
VAM	Vogel's Approximation Method
MCS	Modulation and Coding Scheme
CVaR	Conditional Value at Risk
CAGR	Cumulative Average Growth Rate
C-RAN	Cloud Radio Access Network

The authors of [16]–[18] present a resilient frame formation for multiplexing the provisions of different users. In [16], the authors jointly MBB and mission-critical communication traffic by engaging dynamic TDD and TTI. In [17], the authors represent tractable multiplexing of mobile broadband (MBB), massive machine communication (MCC), and mMTC considering dynamic TTI. The authors of [18] present a holistic overview of the agile scheduling for 5G that incorporates multiple users. They envision an E2E QoS architecture to offer improved opportunities for application-layer scheduling functionality that ensures QoE for each user. $M/D/m/m$ queueing model-based system-level design has proposed for fulfilling $uRLLC$ traffic demand in [19], where they exhibit that the static bandwidth partitioning is inefficient for $eMBB$ and $uRLLC$ traffic. Thus, the authors of [19] have illustrated

a dynamic mechanism for multiplexing of $eMBB$ and $uRLLC$ traffic and apply this in both frequency and time domain.

The efficient way of network resource sharing for the $eMBB$ and $uRLLC$ is studied in [20]. A dynamic puncturing mechanism is proposed for $uRLLC$ traffic in [20] within $eMBB$ resources to increase the overall resource utilization in the network. To enhance the performance for decoding of $eMBB$ traffic, a joint signal space diversity and dynamic puncturing schemes have proposed, where they improve the performance of component interleaving as well as rotation modulation. For reducing the queuing delay of the $uRLLC$ traffic, the authors introduce punctured scheduling (PS) in [21]. In case of insufficient radio resource availability, the scheduler promptly overwrites a portion of the $eMBB$ transmission by the $uRLLC$ traffic. The scheduler improves the $uRLLC$ latency performance; however, the performance of the $eMBB$ users are profoundly deteriorated. The authors of [22] and [23] manifest the coexistence technique for enabling 5G wireless services like $eMBB$ and $uRLLC$ based upon a punctured scheme. The authors present an enhanced PS (EPS) scheduler to enable an improved ergodic capacity of the $eMBB$ users in [24]. EPS is capable of recovering the lost information due to puncturing and partially. $eMBB$ users are supposed to be cognizant about the corresponding resource that is being penetrated by $uRLLC$. Therefore, the victim $eMBB$ users ignore the punctured resources from the erroneous chase condensing HARQ process. The authors of [25] propose a MUPS, where they discretize the trade-off among network system capacity and $uRLLC$ performance. MUPS first tries to match the incoming $uRLLC$ traffic inside an $eMBB$ traffic in a conventional multi-user multiple-input multiple-output (MU-MIMO) transmission. MUPS serves the $uRLLC$ traffic instantly by using PS if MU pairing cannot be entertained immediately. Though MUPS shows improved spectral efficiency, it is not feasible for $uRLLC$ latency as MU pairing mostly depends on the rate maximization. Hence, the inter-user interference can further degrade the signal-to-interference-noise-ratio (SINR) quality of the $uRLLC$ traffic, which can lead to reliability concerns. The authors of [26] propose a null-space-based preemptive scheduler (NSBPS) for jointly serving $uRLLC$ and $eMBB$ traffic in a densely populated 5G arrangement. The proposed approach ensures on-the-spot scheduling for the sporadic $uRLLC$ traffic, while makes a minimal shock on the overall system outcome. The approach employs the system spatial degrees of freedom (SDoF) for $uRLLC$ traffic for spontaneously providing a noise-free subspace.

In [27], a joint scheduling problem is formulated for $eMBB$ and $uRLLC$ traffic in the goal of maximizing $eMBB$ users' utility while satisfying stochastic demand for the $uRLLC$ UEs. Specifically, they measure the loss of $eMBB$ users for superposition/puncturing by introducing three models, which include linear, convex and threshold-based schemes. In [28], the authors propose a non-orthogonal coexistence scheme for $uRLLC$ and $eMBB$ services by processing $uRLLC$ traffic at the edge nodes, whereas $eMBB$ traffic is controlled centrally at the cloud. They analyze both uplink and downlink scenario considering the heterogeneous requirements of those traffic. In [29], the authors present a risk-sensitive approach for

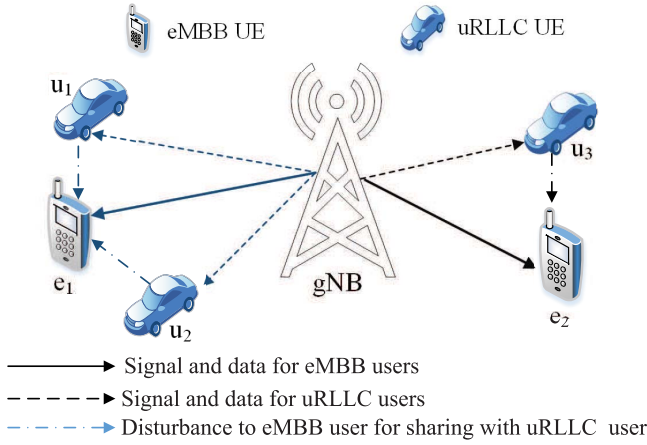


Fig. 1. System model for coexisting *e*MBB and *u*RLLC services in 5G. e_1 is sharing RBs with u_1 and u_2 , and hence, creating capacity loss for e_1 . e_2 is sharing RBs with u_3 , and hence, creating capacity loss for e_2 .

allocating resource blocks (RBs) to *u*RLLC traffic in the goal of minimizing the uncertainty of *e*MBB transmission. Particularly, they launch the Conditional Value at Risk (CVaR) for estimating the uncertainty of *e*MBB traffic.

III. SYSTEM MODEL AND PROBLEM FORMULATION

In this work, we consider a 5G network scenario with one next generation base station (gNB) which supports a group of user equipment (UE) \mathcal{E} requiring *e*MBB service, and a set of user equipment \mathcal{U} demanding *u*RLLC service. Like most of the works in literature, e.g. [20]–[27], we considered a scenario with downlink transmissions from a common gNB to UEs using different services (i.e., *e*MBB and *u*RLLC), and the overall system diagram is shown in Fig. 1. gNB supports the UEs using licensed RBs \mathcal{K} each with equal bandwidth of B . Every time slot, with a length Δ , is split into M mini-slots of duration δ for managing low latency services. For supporting *e*MBB UEs, we consider T_s LTE time slots and denoted by $\mathcal{T} = \{1, 2, \dots, T_s\}$. *u*RLLC traffic arrive at gNB (any mini-slot m of time slot t) follows Gaussian distribution, i.e., $U \sim \mathcal{N}(\mu, \sigma^2)$. Here, μ and σ^2 denote the mean and variance of U . Each *u*RLLC UE $u \in \mathcal{U}$ request for a payload of size $L_u^{m,t}$ (varying from 32 to 200 Bytes [30]).

gNB allots the RBs to the *e*MBB UEs at the commencement of any time slot $t \in \mathcal{T}$. The achievable rate of $e \in \mathcal{E}$ for RB $k \in \mathcal{K}$ is as follows:

$$r_{e,k}^t = \Delta B \log_2(1 + \gamma_{e,k}^t), \quad (1)$$

where $\gamma_{e,k}^t = \frac{P_e h_e^2}{N_0 B}$ presents signal-to-noise-ratio (SNR). However, in our mathematical modeling of the system, we considered the residual interference generated by adjacent gNBs to be negligible assuming that an interference avoidance technique (e.g. using disjoint sets of sub-channels for neighboring cells) [31] can keep the inter-cell interference to minimal levels. The overview of the generalization process of the proposed model into multicell model is presented in Appendix. P_e is the transmission power of gNB for $e \in \mathcal{E}$ and h_e denotes the gain of $e \in \mathcal{E}$ from the gNB, and N_0 represents the noise

TABLE II
SUMMARY OF NOTATIONS

Symbol	Meaning
\mathcal{E}	Set of active <i>e</i> MBB users
\mathcal{U}	Set of <i>u</i> RLLC users
\mathcal{K}	Set of RBs of uniform bandwidth B
B	Bandwidth of a RB
Δ	Duration of a time slot
δ	Duration of a mini-slot
M	Number of mini-slots in a time slot
T	Total number of time slots
λ	Mean value of arrival rate of <i>u</i> RLLC traffic
U	Random number representing arrival rate of traffics for <i>u</i> RLLC users at mini-slot m of time slot t
$L_u^{m,t}$	Payload size of <i>u</i> RLLC user $u \in \mathcal{U}$ at mini-slot m of time slot t
γ_e^t	SNR of <i>e</i> MBB user $e \in \mathcal{E}$ in time slot t
P_e	Transmission power of gNB for <i>e</i> MBB user $e \in \mathcal{E}$
h_e	Channel gain of for <i>e</i> MBB user $e \in \mathcal{E}$ from gNB
N_0	Noise spectral density
α	Resource allocation vector for \mathcal{E}
$\gamma_u^{m,t}$	SINR/SNR of <i>u</i> RLLC user $u \in \mathcal{U}$ from gNB at mini-slot m of time slot t
P_u	Transmission power of gNB for <i>u</i> RLLC user $u \in \mathcal{U}$
h_u	Channel gain of for <i>u</i> RLLC user $u \in \mathcal{U}$ from gNB
V_u	Channel dispersion for <i>u</i> RLLC user u
N_u^b	Blocklength of <i>u</i> RLLC traffic from user u
Q	Complementary Gaussian cumulative distribution function
ε_u^d	Probability of decoding error for <i>u</i> RLLC user u
β	Resource allocation vector for \mathcal{U}
ϕ	Vector for representing current serving <i>u</i> RLLC users
ϵ	<i>u</i> RLLC reliability probability
$r_{e,k}^t$	Achievable rate of <i>e</i> MBB user e in RB k of time slot t
$r_{u,k}^{m,t}$	Achievable rate of <i>u</i> RLLC user u in RB k at mini-slot m of time slot t
σ	Standard deviation of incoming <i>u</i> RLLC traffic in any mini-slot
μ	Mean of incoming <i>u</i> RLLC traffic in any mini-slot

spectral density. *e*MBB UEs require more than one RB for satisfying their QoS. Therefore, the achievable rate of *e*MBB UE $e \in \mathcal{E}$ in time slot t is as follows:

$$r_e^t = \sum_{k \in \mathcal{K}} \alpha_{e,k}^t r_{e,k}^t, \quad (2)$$

where α denotes the resource allocation vector for \mathcal{E} at any time slot t , and each element is as follows:

$$\alpha_{e,k}^t = \begin{cases} 1, & \text{if RB } k \text{ is allocated for } e \in \mathcal{E} \text{ at time slot } t, \\ 0, & \text{otherwise.} \end{cases} \quad (3)$$

*u*RLLC traffic can arrive at some moment (i.e. mini-slot) inside any time slot t and requires to be attended quickly. Any *u*RLLC traffic needs to be completed within a mini-slot

period for its' latency and reliability constraints. Normally, the payload size of *uRLLC* traffic is really short, and therefore, we cannot straightforwardly adopt Shannon's data rate formulation [10]. The achievable rate of a *uRLLC* UE $u \in \mathcal{U}$ in RB $k \in \mathcal{K}$, when its' traffic is overlapped with *eMBB* traffic, can properly be approximated by employing [32] as follows:

$$r_{u,k}^{m,t} = \delta \left[B \log_2(1 + \gamma_u^{m,t}) - \sqrt{\frac{V_u}{N_u^b}} Q^{-1}(\varepsilon_u^d) \right], \quad (4)$$

where $\gamma_u^{m,t} = \frac{h_u^2 P_u}{N_0 B + h_u^2 P_e}$ represents the SINR for $u \in \mathcal{U}$ at mini-slot m of t . Here, $h_u^2 P_e$ indicates the interference generated from serving $e \in \mathcal{E}$ in the same RB, $V_u = \frac{h_u^2 P_u}{N_0 B + h_u^2 (P_u + P_e)}$ depicts the channel dispersion, and meaning of other symbols are shown in II. However, the reliability of *uRLLC* traffic fall into vulnerability due to the interference. Hence, superposition mechanism is not a suitable for serving *uRLLC* UE [11]. Thus, for serving *uRLLC* UEs, we concentrate on the puncturing technique. In the punctured mini-slot, gNB allots zero power for *eMBB* UE, and therefore, the interference cannot affect the *uRLLC* traffic. At that time, $\gamma_u^{m,t} = \frac{h_u^2 P_u}{N_0 B}$ and $V = \frac{h_u^2 P_u}{N_0 B + h_u^2 P_u}$. The achieved rate of $u \in \mathcal{U}$, when it uses multiple RBs, is as follows:

$$r_u^{m,t} = \sum_{k \in \mathcal{K}} \beta_{e,k}^{m,t} r_{u,k}^{m,t}, \quad (5)$$

where β is the resource allocation vector for \mathcal{U} at m of t , and each of its' element follows:

$$\beta_{e,k}^{m,t} = \begin{cases} 1, & \text{if RB } k \text{ is allocated for } u \in \mathcal{U} \text{ at } m \text{ of } t, \\ 0, & \text{otherwise.} \end{cases} \quad (6)$$

All the *uRLLC* request in any m of t needs to be served for sure, and hence,

$$P\left(\sum_{u \in \mathcal{U}} \phi_u^{m,t} < U\right) \leq \epsilon, \quad \forall m, t. \quad (7)$$

where ϕ denotes a vector for the serving *uRLLC* UEs, and thus,

$$\phi_u^{m,t} = \begin{cases} 1, & \text{if } u \in \mathcal{U} \text{ is served by the gNB at } m \text{ of } t, \\ 0, & \text{otherwise.} \end{cases} \quad (8)$$

Within the stipulated period δ , the payload $L_u^{m,t}$ of $u \in \mathcal{U}$ needs to be transferred, and hence, satisfy the following:

$$\phi_u^{m,t} L_u^{m,t} \leq \delta r_u^{m,t}, \quad \forall u, m, t. \quad (9)$$

Hence, the reliability and latency requirements of *uRLLC* traffic are respectively considered in (7) and (9). Besides, $e \in \mathcal{E}$ loses some throughput at t if *uRLLC* traffic is punctured within its' RBs. We consider that the *eMBB* rate loss associated with URLLC puncturing is directly proportional to the fraction of punctured minislots. This linear proportional is motivated by basic results for the channel capacity of AWGN channel with erasures, see [44] for more details. Our system in a given network state can be approximated as an AWGN channel with erasures, when the slot sizes are long enough so that the physical layer error control coding of *eMBB* users use long code-words. Further, there is a dedicated

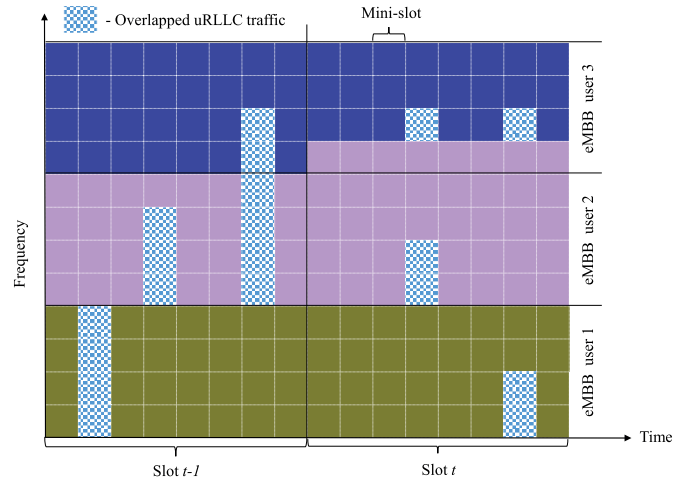


Fig. 2. Example of multiplexing between *eMBB* and *uRLLC* traffic.

control channel through which the scheduler can signal to the *eMBB* receiver indicating the positions of URLLC overlap. Indeed such a control channel has been proposed in the 3GPP standards [4]. We utilize the linear model of [27] for estimating the throughput-losses of *eMBB* UE. Therefore, the throughput-losses $e \in \mathcal{E}$ looks like as follows:

$$r_{e,loss}^t = \sum_{k \in \mathcal{K}} r_{e,k}^t \sum_{m \in \mathcal{M}} \sum_{u \in \mathcal{U}} \mathbb{I}(\alpha_{e,k}^t = \beta_{u,k}^{m,t}). \quad (10)$$

So, the actual achievable rate of $e \in \mathcal{E}$ in any t is as follows:

$$r_{e,actual}^t = r_e^t - r_{e,loss}^t. \quad (11)$$

We see that β affects on α , and hence, impact negatively to the *eMBB* throughput in each $t \in \mathcal{T}$. At the start of any $t \in \mathcal{T}$, gNB allocates the RBs \mathcal{K} among the \mathcal{E} in an orthogonal fashion as shown in Fig. 2. These characteristics of α are shown mathematically as follows:

$$\sum_{e \in \mathcal{E}} \alpha_{e,k}^t \leq 1, \quad \forall k, \quad (12)$$

$$\sum_{k \in \mathcal{K}} \alpha_{e,k}^t \geq 1, \quad \forall e, \quad (13)$$

$$\sum_{e \in \mathcal{E}} \sum_{k \in \mathcal{K}} \alpha_{e,k}^t \leq |\mathcal{K}|. \quad (14)$$

Within each $t \in \mathcal{T}$, gNB allows *uRLLC* UEs to get some RBs immediately on a mini-slot basis. Therefore, *uRLLC* traffic overlaps with *eMBB* traffic at m and also shown in Fig. 2. Accordingly, β satisfy the following conditions on each m :

$$\sum_{u \in \mathcal{U}} \beta_{u,k}^{m,t} \leq 1, \quad \forall k, \quad (15)$$

$$\sum_{k \in \mathcal{K}} \phi_u^{m,t} \beta_{u,k}^{m,t} \geq 1, \quad \forall u, \quad (16)$$

$$\sum_{u \in \mathcal{U}} \sum_{k \in \mathcal{K}} \phi_u^{m,t} \beta_{u,k}^{m,t} \leq |\mathcal{K}|. \quad (17)$$

Finally, our objective is to maximize the actual achievable rate of each *eMBB* UE across \mathcal{T} while entertaining nearly

every *uRLLC* request within its' speculated latency. We apply *Max-Min* fairness doctrine for this mission, and it contributes stationary service quality, enhances spectral efficiency and makes UEs more pleasant in the network. Hence, the maximization problem is formulated as follows:

$$\max_{\alpha, \beta} \min_{e \in \mathcal{E}} \mathbb{E} \left(\sum_{t=1}^{|\mathcal{T}|} r_{e, actual}^t \right) \quad (18)$$

$$\text{s.t. } P \left(\sum_{u \in \mathcal{U}} \phi_u^{m,t} < U \right) \leq \epsilon, \quad \forall m, t, \quad (18a)$$

$$\phi_u^{m,t} L_u^{m,t} \leq \delta r_u^{m,t}, \quad \forall u, m, t, \quad (18b)$$

$$\sum_{e \in \mathcal{E}} \alpha_{e,k}^t \leq 1, \quad \forall k, t, \quad (18c)$$

$$\sum_{u \in \mathcal{U}} \beta_{u,k}^{m,t} \leq 1, \quad \forall k, m, t, \quad (18d)$$

$$\sum_{k \in \mathcal{K}} \alpha_{e,k}^t \geq 1, \quad \forall e, t, \quad (18e)$$

$$\sum_{k \in \mathcal{K}} \phi_u^{m,t} \beta_{u,k}^{m,t} \geq 1, \quad \forall u, m, t, \quad (18f)$$

$$\sum_{e \in \mathcal{E}} \sum_{k \in \mathcal{K}} \alpha_{e,k}^t + \sum_{u \in \mathcal{U}} \sum_{k \in \mathcal{K}} \phi_u^{m,t} \beta_{u,k}^{m,t} \leq |\mathcal{K}|, \quad \forall t, \quad (18g)$$

$$\alpha_{e,k}^t, \beta_{u,k}^{m,t}, \phi_u^{m,t} \in \{0, 1\}, \quad \forall e, u, k, m, t. \quad (18h)$$

In (18), the reliability and latency constraints of the *uRLLC* UEs are preserved by (18a) and (18b). Constraints (18c) and (18d) are used to show the orthogonality of RBs among *eMBB* and *uRLLC* UEs, respectively. At least one RB is posed by every active UE and is encapsulated by both (18e) and (18f). Resource restriction is presented by constraint (18g). Constraint (18h) shows that every item of α , β and ϕ are binary. The formulation (18) is a Combinatorial Programming (CP) problem having chance constraint, and NP-hard due to its nature.

IV. DECOMPOSITION AS A SOLUTION APPROACH FOR PROBLEM (18)

We assume that *eMBB* UEs are data-hungry over the considered period. Thus, at the commencement of a time slot $t \in \mathcal{T}$, gNB schedules all of its' RBs among the *eMBB* UEs and stay unchanged over t . If *uRLLC* traffic requests come in any m of t , the scheduler tries to serve the requests in the next $m+1$. Hence, the overlapping of *uRLLC* traffic over *eMBB* traffic happens as shown in Fig. 2. Usually, a portion of all RBs is required for serving such *uRLLC* traffic. However, the challenge is to find the victimized *eMBB* UE(s) following the aspiration of the problem (18).

For getting an effective solution to the problem (18), we can utilize the concept of a divide-and-conquer strategy. Here, we divide (18) into two resource allocation sub-problems, namely, for *eMBB* UEs on time slot basis and *uRLLC* UEs on a mini-slot basis. The first sub-problem is as follows:

$$\max_{\alpha} \min_{e \in \mathcal{E}} \mathbb{E} \left(\sum_{t=1}^{|\mathcal{T}|} r_{e, actual}^t \right) \quad (19)$$

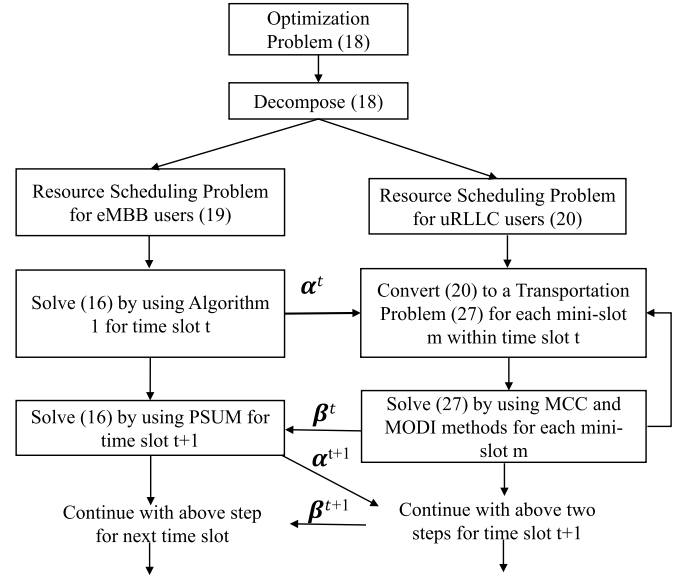


Fig. 3. Overview of the solution process for (18).

$$\text{s.t. } \sum_{e \in \mathcal{E}} \alpha_{e,k}^t \leq 1, \quad \forall k, t, \quad (19a)$$

$$\sum_{k \in \mathcal{K}} \alpha_{e,k}^t \geq 1, \quad \forall e, t, \quad (19b)$$

$$\sum_{e \in \mathcal{E}} \sum_{k \in \mathcal{K}} \alpha_{e,k}^t \leq |\mathcal{K}|, \quad \forall t, \quad (19c)$$

$$\alpha_{e,k}^t \in \{0, 1\}, \quad \forall e, k, t. \quad (19d)$$

On the other hand, the second sub-problem (with $\alpha^t, \forall t$ as the solution of 19) is manifested as follows:

$$\max_{\beta} \min_{e \in \mathcal{E}} \mathbb{E} \left(\sum_{t=1}^{|\mathcal{T}|} r_{e, actual}^t \right) \quad (20)$$

$$\text{s.t. } P \left(\sum_{u \in \mathcal{U}} \phi_u^{m,t} < U \right) \leq \epsilon, \quad \forall m, t, \quad (20a)$$

$$\phi_u^{m,t} L_u^{m,t} \leq \delta r_u^{m,t}, \quad \forall u, m, t, \quad (20b)$$

$$\sum_{u \in \mathcal{U}} \beta_{u,k}^{m,t} \leq 1, \quad \forall k, m, t, \quad (20c)$$

$$\sum_{k \in \mathcal{K}} \phi_u^{m,t} \beta_{u,k}^{m,t} \geq 1, \quad \forall u, m, t, \quad (20d)$$

$$\sum_{u \in \mathcal{U}} \sum_{k \in \mathcal{K}} \phi_u^{m,t} \beta_{u,k}^{m,t} \leq |\mathcal{K}|, \quad \forall m, t, \quad (20e)$$

$$\beta_{u,k}^{m,t}, \phi_u^{m,t} \in \{0, 1\}, \quad \forall u, k, m, t. \quad (20f)$$

Fig. 3 shows the solution overview of the optimization problem (18). We can better understand the philosophy of the problem and the solution approach with an illustrative example in Fig. 2. At the beginning of the time slot, $t-1$, let us assume that there are 3 *eMBB* UEs, each of whom owns 4 RBs. Within $t-1$, the service request for *uRLLC* UEs came abruptly and the allocation of RBs for that UEs is shown in Fig. 2, as overlapped *uRLLC* traffic in the mini-slots.

During this time, *eMBB* users 1, 2 and 3 waste throughput equivalent to $4\text{RBs} \times 1$ mini-slot, $7\text{RBs} \times 1$ mini-slot, and $2\text{RBs} \times 1$ mini-slot, respectively. At the start of the next time slot, t , gNB acknowledges the resource scheduling of *uRLLC* UEs of $t - 1$ to allocate and compensate *eMBB* UEs. gNB allocates more RBs to *eMBB* user 2 and less to *eMBB* user 3 as they lose more and less, respectively, in the time slot $t - 1$. Moreover, EgNB tries to serve *uRLLC* users such that the loss of throughput of *eMBB* users are almost similar in the time slot t . Therefore, gNB makes a balance among the throughput of *eMBB* users in each time slot, which ultimately serves to reach the goal of (18) on a long-run basis.

A. PSUM as a Solution of the Sub-Problem (19)

Problem (19) is still is computationally expensive to reach a globally optimal solution due to its' NP-hardness. In this sub-section, we propose the *PSUM* algorithm to solve (19) approximately with low complexity. Relaxation of the binary variable and the addition of a penalty term to the objective function is the main philosophy of our proposed *PSUM* algorithm. We redefine (19) as follows:

$$\min_{\alpha^t} \sum_{e \in \mathcal{E}} W_e^t(\alpha^t), \quad \forall t, \quad (21)$$

$$\text{s.t. (19a), (19b), (19c),} \quad (21a)$$

$$W_e^t(\alpha^t) = \left| \frac{1}{t|\mathcal{E}|} \sum_{e' \in \mathcal{E}} \left(\sum_{t'=1}^{t-1} r_{e', \text{actual}}^{t'} + r_e^t \right) - \frac{1}{t} \left(\sum_{t'=1}^{t-1} r_{e, \text{actual}}^{t'} + r_e^t \right) \right|, \quad (21b)$$

$$\alpha_{e,k}^t \in [0, 1], \quad \forall e, k, t. \quad (21c)$$

Now according to Theorem 2 of [33], if $|\mathcal{K}|$ is sufficiently large then original sub-problem (19) and (21) are equivalent. Moreover, we add a penalty term L_p to the objective function to get binary solution of relaxed variable from (21). Let $\alpha_k^t = \{\alpha_{e,k}^t\}_{e \in \mathcal{E}}$ and we can rewrite (19a) as $\|\alpha_k^t\|_1 \leq 1, \forall t, k$. The penalized problem is as follows:

$$\min_{\alpha^t} \sum_{e \in \mathcal{E}} W_e^t(\alpha^t) + \sigma P_\varepsilon(\alpha^t), \quad \forall t \quad (19)$$

$$\text{s.t. (21a), (21b), (21c),} \quad (22a)$$

where $\sigma > 0$ is the penalty parameter,

$$P_\varepsilon(\alpha^t) = \sum_{k \in \mathcal{K}} (\|\alpha_k^t + \varepsilon \mathbf{1}\|_p^p - c_{\varepsilon,k}). \quad (23)$$

with $p \in (0, 1)$, and ε is any non-negative constant. Following the fact of [34] which is further described in [33], the optimal value is as follows:

$$c_{\varepsilon,k} = (1 + \varepsilon)^p + (|\mathcal{E}| - 1)\varepsilon^p. \quad (24)$$

Generally, the parameter σ should big enough to make the values of $\{\alpha_{e,k}^t\}$ near zero or one. Then, we achieve a feasible solution of (22) by applying the rounding process.

Algorithm 1 Solution of (19) for Each t Based on *PSUM*

```

1: Initialization:  $\varepsilon_1, \sigma_1, I_{max}$  and let  $i = 0$ 
2: Solve problem (21) and obtain solution  $\alpha^{t,0}$ 
3: while  $i < I_{max}$  do
4:   Set  $\varepsilon = \varepsilon_{i+1}$  and  $\sigma = \sigma_{i+1}$ 
5:   Solve problem (26) with the initial point being  $\alpha^{t,i}$ , and
     obtain a new solution  $\alpha^{t,i+1}$ 
6:   if  $\alpha^{t,i+1}$  is binary then
7:     Stop
8:   else
9:     Set  $i = i + 1$ 
10:    Update  $\varepsilon_{i+1} = \eta\varepsilon$ , and  $\sigma_{i+1} = \zeta\sigma$ 
11:   end if
12: end while

```

It is not easy to solve (22) directly. However, by utilizing the successive upper bound minimization (SUM) technique [35], [36], we can efficiently resolve (22). This method tries to secure the lower bound of the actual objective function by determining a sequence of approximation of the objective functions. As $P_\varepsilon(\alpha^t)$ is concave in nature and hence,

$$P_\varepsilon(\alpha^t) \leq P_\varepsilon(\alpha^{t,i}) + \nabla P_\varepsilon(\alpha^{t,i})^T (\alpha^t - \alpha^{t,i}), \quad (25)$$

where $\alpha^{t,i}$ is the value of current allocation of iteration i . At the $(i+1)$ -th iteration of t , we solve the following problem:

$$\min_{\alpha^t} \sum_{e \in \mathcal{E}} W_e^t(\alpha^t) + \sigma_{i+1} \nabla P_\varepsilon(\alpha^{t,i})^T \alpha^t \quad (26)$$

$$\text{s.t. (21a), (21b), (21c).} \quad (26a)$$

In each iteration, we can get a globally optimal solution for sub-problem (26) by using the solver. Algorithm 1 shows the proposed mechanism for solving (19). In this Algorithm, $0 < \eta < 1 < \zeta$ where ζ and η represent two constants defined previously.

B. Solution of Sub-Problem (20) Through TM

Due to the existence of chance constraint (20a) and also the combinatorial variable, β , (20) is still difficult to resolve by using traditional optimizer. Now, we need to transmute (20a) into deterministic form for solving (20). Moreover, let us assume $g(\phi, U) = \sum_{u \in \mathcal{U}} \phi_u^{m,t} - U$, $U \in \mathbb{R}$ and $U \sim \mathcal{N}(\mu, \sigma^2), \forall m, t$ and hence,

$$\begin{aligned} & Pr\{g(\phi, U) \leq 0\} \\ &= Pr\left\{ \sum_{u \in \mathcal{U}} \phi_u^{m,t} - U \leq 0 \right\} \end{aligned} \quad (27)$$

$$= Pr\left\{ \sum_{u \in \mathcal{U}} \phi_u^{m,t} \leq U \right\} \quad (27a)$$

$$= 1 - Pr\left\{ \sum_{u \in \mathcal{U}} \phi_u^{m,t} \geq U \right\} \quad (27b)$$

$$= 1 - Pr\left\{ \frac{U - \mu}{\sigma} \leq \frac{\sum_{u \in \mathcal{U}} \phi_u^{m,t} - \mu}{\sigma} \right\} \quad (27c)$$

$$= 1 - F_U\left(\sum_{u \in \mathcal{U}} \phi_u^{m,t} \right). \quad (27d)$$

Here, F_U is the cumulative distribution function (CDF) of random variable U . Thus, from constraint (20a), we can rewrite as follows:

$$\Pr\{g(\phi, U) \leq 0\} \geq \epsilon, \quad (28)$$

$$1 - F_U\left(\sum_{u \in \mathcal{U}} \phi_u^{m,t}\right) \leq \epsilon, \quad (28a)$$

$$F_U\left(\sum_{u \in \mathcal{U}} \phi_u^{m,t}\right) \geq 1 - \epsilon, \quad (28b)$$

$$\sum_{u \in \mathcal{U}} \phi_u^{m,t} \geq F_U^{-1}(1 - \epsilon), \quad (28c)$$

$$\sum_{u \in \mathcal{U}} \phi_u^{m,t} - F_U^{-1}(1 - \epsilon) \geq 0. \quad (28d)$$

Now, (28d) and (20a) are identical. Hence, the renewed form of (20) looks like as follows:

$$\min_{\beta^t} \sum_{e \in \mathcal{E}} V_e^t(\alpha^t, \beta^t), \quad \forall t \quad (29)$$

$$\text{s.t.} \quad \sum_{u \in \mathcal{U}} \phi_u^{m,t} - F_U^{-1}(1 - \epsilon) \geq 0, \quad \forall m, \quad (29a)$$

$$(20b), (20c), (20d), (20e), (20f), \quad \forall u, m, \quad (29b)$$

$$V_e^t(\alpha^t, \beta^t) = \left| \frac{1}{|\mathcal{E}|} \sum_{e' \in \mathcal{E}} r_{e',loss}^t - r_{e,loss}^t \right|, \quad \forall e. \quad (29c)$$

Problem (29) is still NP-hard due to the appearance of combinatorial variable. In (29), (29a) holds for a particular value of ϵ when gNB serves a certain portion of uRLLC UE $U' \leq U$. For a m of t , let us assume $U' = \{1, 2, \dots, U'\}$ and $\phi_u^{m,t} = 1, \forall u \in U'$. We can determine the requisite RBs, $\forall u \in U'$ holding δ as the upper-bound in (20b) and let $\mathbf{d} = [d_1, d_2, \dots, d_{|U'|}]$. As gNB engages OFDMA for uRLLC UEs, constraint (20c) holds. Moreover, depending on U' , constraints (20d), (20e), and (20f) also hold. Constraint (29c) can be used as a basic block to build a cost matrix $\mathbf{C} = (c_{u,e}), u \in U', e \in \mathcal{E}$. As \mathcal{K} are held by eMBB UEs \mathcal{E} in any time slot $t \in \mathcal{T}$, we can find a vector $\mathbf{s} = [s_1, s_2, \dots, s_{|\mathcal{E}|}]$. Now redefine problem (29) as follows:

$$\min_{\chi} \sum_{u \in U'} \sum_{e \in \mathcal{E}} c_{ue} \chi_{ue} \quad (30)$$

$$\text{s.t.} \quad \sum_{e \in \mathcal{E}} \chi_{ue} = d_u, \quad \forall u \in U', \quad (30a)$$

$$\sum_{u \in U'} \chi_{ue} \leq s_e, \quad \forall e \in \mathcal{E}, \quad (30b)$$

$$\sum_{u \in U'} d_u \leq \sum_{e \in \mathcal{E}} s_e, \quad (30c)$$

$$\sum_{e \in \mathcal{E}} s_e = |\mathcal{K}|, \quad (30d)$$

$$\chi_{ue} \geq 0, \quad \forall u \in U', e \in \mathcal{E}. \quad (30e)$$

The goal of (30) is to find a matrix $\chi \in \mathbb{Z}^{|U'| \times |\mathcal{E}|} = (\chi_{ue}), \forall u \in U', e \in \mathcal{E}$ that will minimize the cost/loss of eMBB UEs. This is a linear programming problem equivalent to the Hitchcock problem [37] with inequities, which contributed to unbalanced transportation model. Introducing slack variables $\chi_{|U'|+1,e}, \forall e \in \mathcal{E}$ and $d_{|U'|+1}$ in the constraints (30b)

and (30c), respectively, which convert them into equality, we have:

$$\sum_{u \in U'} \chi_{ue} + \chi_{|U'|+1,e} = s_e, \quad \forall e \in \mathcal{E}, \quad (31)$$

$$\sum_{u \in U'} d_u + d_{|U'|+1} = \sum_{e \in \mathcal{E}} s_e. \quad (32)$$

Now the modified problem in (30) is a balanced transportation model (*BTM*). Moreover, we have to add $d_{|U'|+1} = \sum_{e \in \mathcal{E}} s_e - \sum_{u \in U'} d_u$ to the demand vector \mathbf{d} as $\mathbf{d} = \mathbf{d} \cup \{d_{|U'|+1}\}$ and a row $[0]_{1 \times |\mathcal{E}|}$ to cost matrix \mathbf{C} as $\mathbf{C} = \mathbf{C} \cup \{[0]_{1 \times |\mathcal{E}|}\}$. *BTM* can be solved by the simplex method [38]. The solution matrix χ will be in the form of $\mathbb{Z}^{(|U'|+1) \times |\mathcal{E}|}$. Northwest corner (*NWC*) [39], *MCC* [39], and Vogel's approximation method (*VAM*) [39], [40] are some of the popular methods for obtaining initial feasible solution of *BTM*. We can use the stepping-stone [41] or *MODI* [42] method to get an optimal solution of the *BTM*. In the following sub-section, we use the combination of the *MCC* and *MODI* for acquiring the optimal result from the *BTM*.

1) *Determining Initial Feasible Solution by MCC Method*: *MCC* method allots to those cells of χ considering the lowest cost from \mathbf{C} . Firstly, the method allows the maximum permissible to the cell with the lowest per RB cost. Secondly, the amount of quantity and need is synthesized while crossing out the satisfied row(s) or column(s). Either row or column is ruled out if both of them are satisfied concurrently. Thirdly, we inquire into the uncrossed-out cells which have the least unit cost and continue it till there is specifically one row or column is left uncrossed. The primary steps of the *MCC* method are compiled as follows:

Step 1: Distribute maximum permissible to the worthwhile cell of χ which have the minimum cost found from \mathbf{C} , and update the supply (s) and demand (d).

Step 2: Continue **Step 1** till there is any demand that needs to be satisfied.

2) *MODI Method for Finding an Optimal Solution*: The initial solution found from section IV-B.1 is used as input in the *MODI* method for finding an optimal solution. We need to augment an extra left-hand column and the top row (indicated by x_u and y_e respectively) with \mathbf{C} whose values require to be calculated. The values are measured for all cells which have the corresponding allocation in χ and shown as follows:

$$x_u + y_e = c_{u,e}, \quad \forall \chi_{u,e} \neq \emptyset. \quad (33)$$

Now we solve (33) to obtain all x_u and y_e . If necessary then assign zero to one of the unknowns toward finding the solution. Next, evaluate for all the empty cells of χ as follows:

$$k_{u,e} = c_{u,e} - x_u - y_e, \quad \forall \chi_{u,e} = \emptyset. \quad (34)$$

Now select $k_{u,e}$ corresponding to the most negative value and determine the stepping-stone path for that cell to know the reallocation amount to the cell. Next, allocate the maximum permissible to the empty cell of χ corresponding to the selected $k_{u,e}$. x_u and y_e values for \mathbf{C} and χ must be recomputed with the help of (33) and a cost change for the empty cells of χ need to be figured out using (34). A corresponding reallocation takes place just like the previous step and the

process continues till there is a negative $k_{u,e}$. At the end of this repetitive process, we get the optimal allocation (χ). The *MODI* method described above can be summed as follows:

Step 1: Develop a preliminary solution (χ) applying the *MCC* method.

Step 2: For every row and column of C , measure x_u and y_e by applying (33) to each cell of χ that has an allocation.

Step 3: For every corresponding empty cell of χ , calculate $k_{u,e}$ by applying (34).

Step 4: Determine the stepping-stone path [41] from χ corresponding to minimum $k_{u,e}$ that found in **Step 3**.

Step 5: Based on the stepping-stone path found in **Step 4**, allocate the highest possible to the free cell of χ .

Step 6: Reiterate **Step 2** to **5** until all $k_{u,e} \geq 0$.

C. Low-Complexity Heuristic Algorithm for Solving Sub-Problem (19)

Though Algorithm 1 can solve the sub-problem (19) optimally, but computation time requires to solve it grows much faster as the size of the problem increase. Besides, the number of *eMBB* UEs is large in reality, and we have a short period to resolve this kind of problem. Therefore, we need a faster and efficient heuristic algorithm, which may sacrifice optimality, to solve (19). Thus, we propose Algorithm 2 for solving (19). At $t = 1$, Algorithm 2 allocate resources equally to the *eMBB* UEs. But, it allocates resources to *eMBB* UEs in the rest of the time slots depending on the proportional loss of the previous time slot. In this way, Algorithm 2 can accommodate the *MEAR* of *eMBB* UEs in the long-run. The complexity of Algorithm 2 depends on \mathcal{T} and \mathcal{E} .

V. NUMERICAL ANALYSIS AND DISCUSSIONS

In this section, we assess the proposed approach using comprehensive experimental analyses. Here, we compare our results with the results of the following state-of-the-art schedulers:

- **PS** [21]: PS immediately overwrite part of the continuing *eMBB* transmission with the sporadic *uRLLC* traffic if there are not sufficient physical resource blocks (PRBs) available. It chooses PRBs with the highest MCS that already been allotted to *eMBB* UEs.
- **MUPS** [25]: In case of insufficient RBs, MUPS allocates PRBs to the *uRLLC* UEs where they endure better channel quality depending on the CQI feedback.
- **RS**: RS takes the RBs from the *eMBB* UEs randomly in case of inadequate PRBs for supporting *uRLLC* traffic.
- **EDS**: For supporting sporadic *uRLLC* traffic, EDS offers the PRBs to this traffic after preempting PRBs equally from the *eMBB* UEs in case of unavailable PRBs.
- **MBS**: gNB uses many to one matching game for snatching PRBs from *eMBB* UEs for supporting *uRLLC* traffic.

The main performance parameters are *MEAR* and fairness [43] of the *eMBB* UEs and defined as follows:

$$\text{MEAR} = \min \mathbb{E} \left(\sum_{t=1}^{|\mathcal{T}|} r_{e,actual}^t \right), \quad \forall e \in \mathcal{E}, \quad (35)$$

Algorithm 2 Heuristic Algorithm for Solving (19)

```

1: Initialization:  $\varepsilon_1, \sigma_1, I_{max}$  and let  $i = 0$ 
2: Solve problem (21) and obtain solution  $\alpha^{t,0}$ 
3: for each  $t \in \mathcal{T}$  do
4:   if  $t = 1$  then
5:     Calculate  $N_{RB} = \frac{|\mathcal{K}|}{|\mathcal{E}|}$ 
6:     for each  $e \in \mathcal{E}$  do
7:       for each  $k = 1 \cdots N_{RB}$  do
8:          $\alpha_{e,(e-1)*N_{RB}+k}^t = 1$ 
9:       end for
10:    end for
11:   else
12:     Determine  $r_{e,loss}^{t-1}$  and  $r_{e,actual}^{t-1}$  for all  $e \in \mathcal{E}$  by using
      (10) and (11) respectively
13:     Set  $loc = 0$ 
14:     for each  $e \in \mathcal{E}$  do
15:       Calculate  $N_{RB}^e = \frac{r_{e,loss}^{t-1}}{\sum_{e' \in \mathcal{E}} r_{e',loss}^{t-1}} |\mathcal{K}|$ 
16:       for each  $k = 1 \cdots N_{RB}^e$  do
17:          $\alpha_{e,loc+k}^t = 1$ 
18:       end for
19:       Set  $loc = loc + N_{RB}^e$ 
20:     end for
21:   end if
22: end for
23: Determine  $r_{e,actual}^t$  for all  $e \in \mathcal{E}$  by using (11)
24: Determine  $\mathbb{E} \left( \sum_{t=1}^{|\mathcal{T}|} r_{e,actual}^t \right)$  for all  $e \in \mathcal{E}$ 

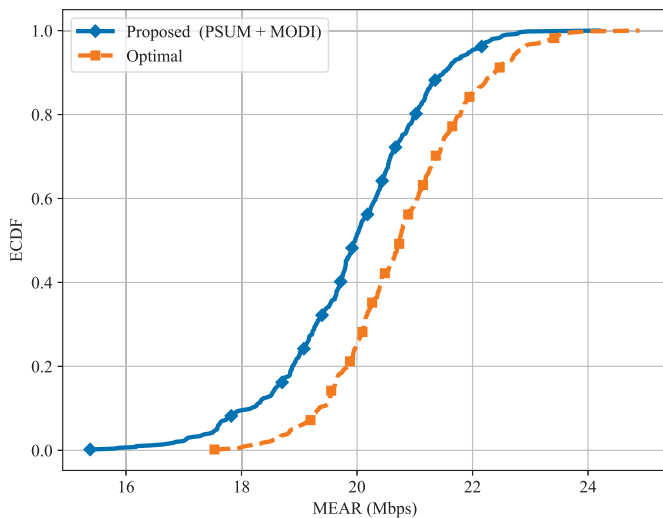
```

$$\text{Fairness} = \frac{\left(\sum_{e \in \mathcal{E}} \mathbb{E} \left(\sum_{t=1}^{|\mathcal{T}|} r_{e,actual}^t \right) \right)^2}{|\mathcal{E}| \cdot \sum_{e \in \mathcal{E}} \left(\sum_{t=1}^{|\mathcal{T}|} r_{e,actual}^t \right)^2}. \quad (36)$$

In our scenario, we consider an area with a radius of 200 m and gNB resides in the middle of the considered area. *eMBB* and *uRLLC* UEs are disseminated randomly in the coverage space. gNB works on a 10 MHz licensed band for supporting the UEs in downlink mode. Every *uRLLC* UE needs a single PRB for its service. Furthermore, gNB estimates path-loss for both *eMBB* and *uRLLC* UEs using a free space propagation model amidst Rayleigh fading. Table III exhibits the significant parameters for this experiment. We use similar *PSUM* parameters as of [33]. Moreover, the values of important simulation parameters of our work follow the 5G NR values as indicated in [45]. The decoding probability of the preempted *eMBB* transmission depends on whether the UE is informed about that or not. If the *eMBB* UE is conscious of the preemption then the performance is surely improved. It can be expedited by granting a preemption indication (PI) to the concerned *eMBB* UEs, such that they understand which RB(s) transmission have been corrupted. The *eMBB* UE(s) benefit from PI information by overlooking the corrupted RBs of the transmission in its decoding process, including potentially performing HARQ soft combining, thereby improving the performance. However, it is fair to compare the proposed method with similar methods i.e. other punctured schemes (without recovery mechanism), and thus, we have compared our method

TABLE III
 SUMMARY OF THE SIMULATION SETUP

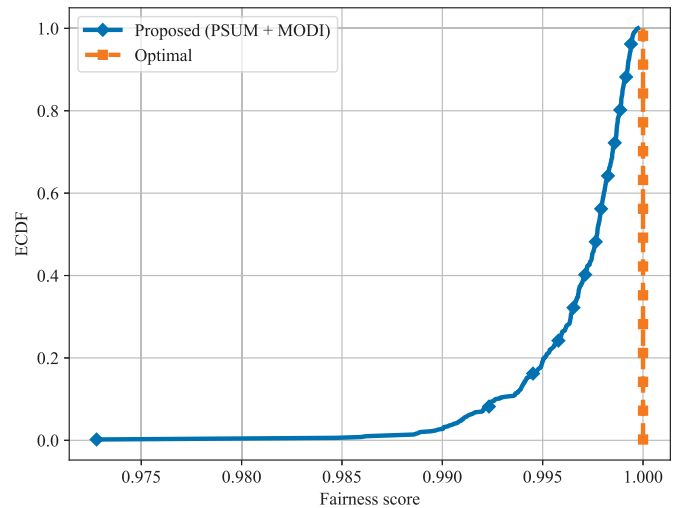
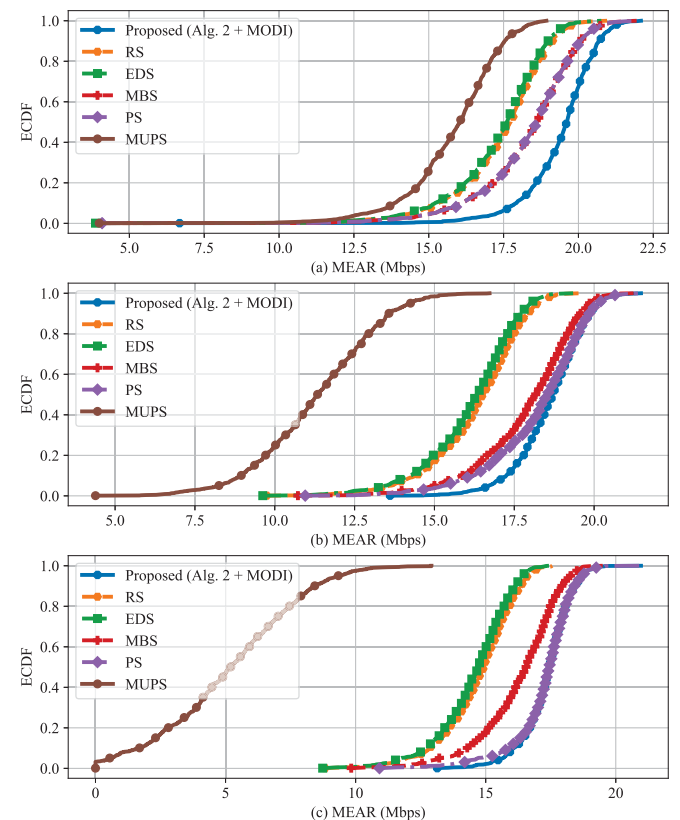
Symbol	Value	Symbol	Value
$ \mathcal{E} $	10	$ \mathcal{K} $	50
B	180 kHz	ϵ	0.00
$ \mathcal{T} $	1000	M	8
Δ	1ms	δ	0.125 ms
$P_e, \forall e$	21 dBm	$P_u, \forall u$	21 dBm
I_{max}	20	N_0	-114 dBm
σ	1, 2, \dots , 10		
L	32, 50, 100, 150, 200 bytes		
eMBB traffic model	Full buffer		
σ_1	2	ϵ_1	0.001
η	0.7	ζ	1.1


 Fig. 4. Comparison of *MEAR* during $\mathcal{E} = 4$ and single *uRLLC* UE in every mini-slot when $L = 32$ bytes.

with such punctured schemes [21], [25], along with other mechanisms. We realize the results of every approaches after taking 1,000 runs.

A comparison of *MEAR* and fairness scores are presented in Fig. 4 and Fig. 5, respectively, between the proposed (*PSUM+TM*) and the optimal value for a small network. Fig. 4 shows the empirical cumulative distribution function (ECDF) of *MEAR* and the probability of *MEAR* being at least 20 Mbps are around 0.50 and 0.70, respectively, for the proposed and optimal methods, consequently. The optimality gap of average *MEAR* for the proposed method is 4.20% as represented in Fig. 4. Fig. 5 shows the ECDF of the fairness scores where the probability of the scores being 0.995 at least is 0.80 in the proposed method in comparison of being 1 in the optimal mechanism. The optimality gap of the proposed method for the average fairness score is 0.32% as exposed from Fig. 5.

For growing *uRLLC* arrivals, the ECDF of the *MEAR* values is exhibited in Fig. 6. Fig. 6 reveals the results that are preferred to those of the other considered methods. The probability of *MEAR* values for being at least 18.0 Mbps are


 Fig. 5. Comparison of fairness score when $\mathcal{E} = 4$ and single *uRLLC* UE in each mini-slot along with $L = 32$ bytes.

 Fig. 6. Comparison of *MEAR* for (a) $\sigma = 1$, (b) $\sigma = 5$, and (c) $\sigma = 10$, along with $L = 32$ Bytes.

0.889, 0.405, 0.367, 0.653, 0.653, and 0.052 for the proposed, RS, EDS, MBS, PS, and MUPS methods, respectively, that are shown in Fig. 6(a). Fig. 6(b) reveals that the likelihood of *MEAR* values for obtaining a minimum of 18.0 Mbps are 0.736, 0.089, 0.050, 0.541, and 0.647 for the proposed, RS, EDS, MBS, and PS methods, respectively, while the MUPS method can accommodate under 18 Mbps in every case. Fig. 6(c) shows that the proposed, MBS and PS methods provide a minimum *MEAR* value of 18.0 Mbps with a probability 0.231, 0.089, and 0.231, respectively, while RS,

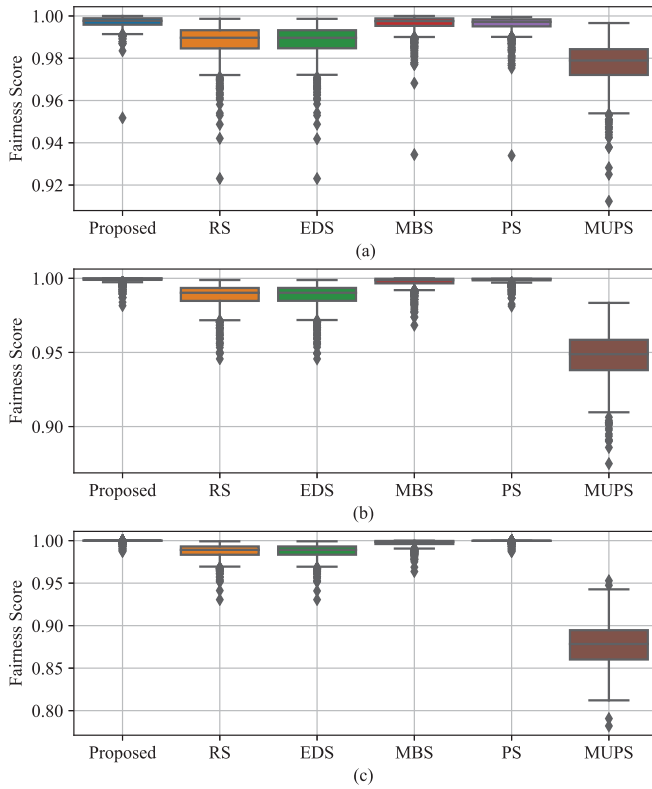


Fig. 7. Comparison of fairness scores (a) $\sigma = 1$, (b) $\sigma = 5$, and (c) $\sigma = 10$, along with $L = 32$ Bytes.

EDS, and MUPS can produce less than 18 Mbps for sure. Moreover, the *MEAR* value decreases with the growing rate of σ for all the methods because of the requirement of more RBs for the *uRLLC* UEs as shown in Fig. 6. But, the increasing arrivals of *uRLLC* traffic affect the MUPS method more as they require extra RBs from the distant *eMBS* UEs. However, the performance gap between the proposed and PS method reduces with the increased arrival of *uRLLC* traffic, as the PS scheme gets more chance to adjust the users with the higher expected achieved rate.

We compare the fairness scores among various methods with different values of σ which is shown in Fig. 7. The scores originating from the proposed method are greater than or similar to that of others as indicated in Fig. 7. Fig. 7(a) reveals that the median of the scores for the proposed, RS, EDS, MBS, PS, and MUPS methods are 0.9977, 0.9897, 0.9897, 0.9975, 0.9972, and 0.9789, respectively. The similar scores are 0.9998, 0.9902, 0.9902, 0.9987, 0.9995, 0.9488, and 1.00, 0.9891, 0.9891, 0.9985, 0.9998, 0.8784 for the corresponding methods and are presented in Fig. 7(b) and 7(c), respectively. Moreover, the fairness scores increase for the Proposed, MBS and PS methods with the increasing value of σ as it gets more chance to maximize the minimum achieved rate, whereas the same scores decrease with the increasing value of σ for RS, EDS and MUPS as *eMBS* UEs have more opportunity to be affected by the *uRLLC* UEs.

Fig. 8 and 9, respectively, show the average *MEAR* and fairness score for varying value of σ . In Fig. 8, we find that our method overpasses other schemes for different rates of σ in

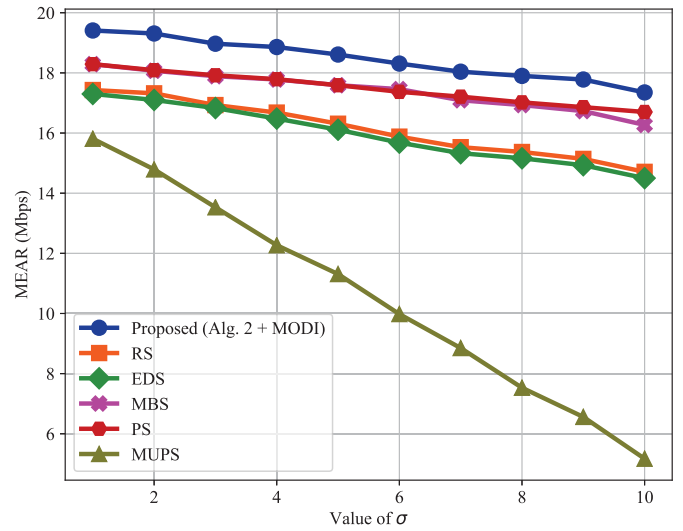


Fig. 8. Comparison of average *MEAR* with varying value of σ and $L = 32$ Bytes.

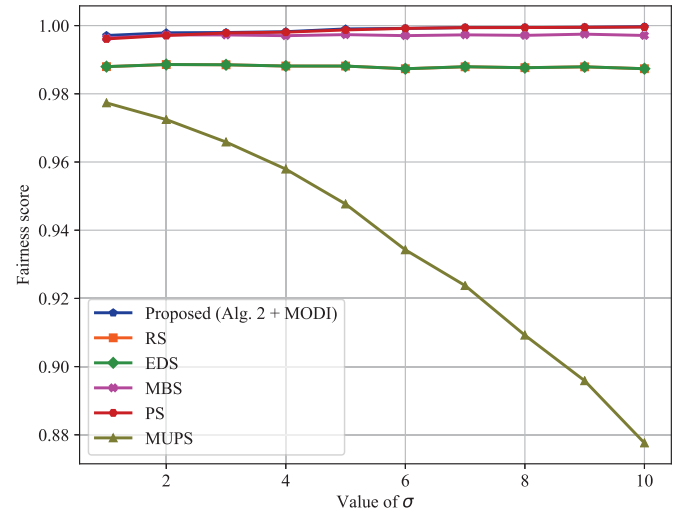
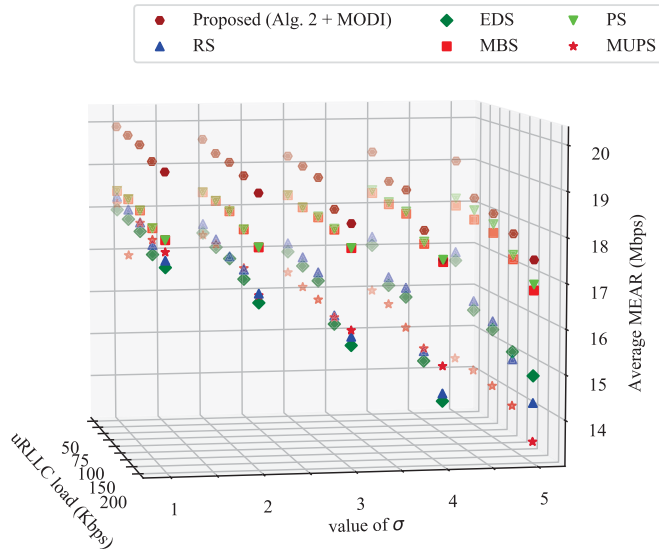
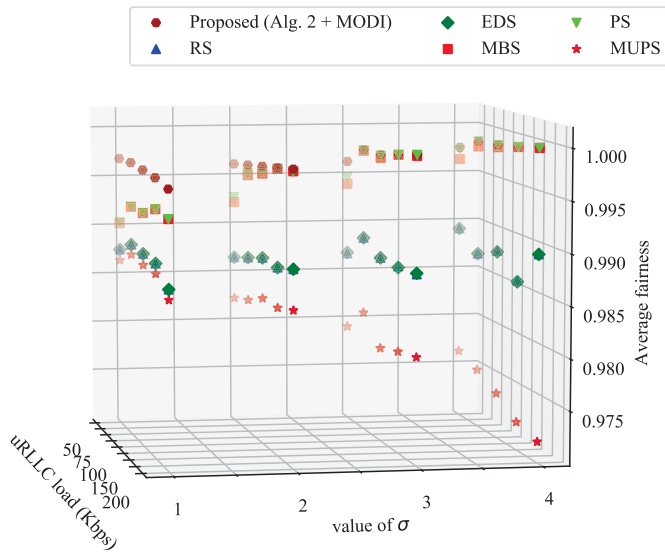


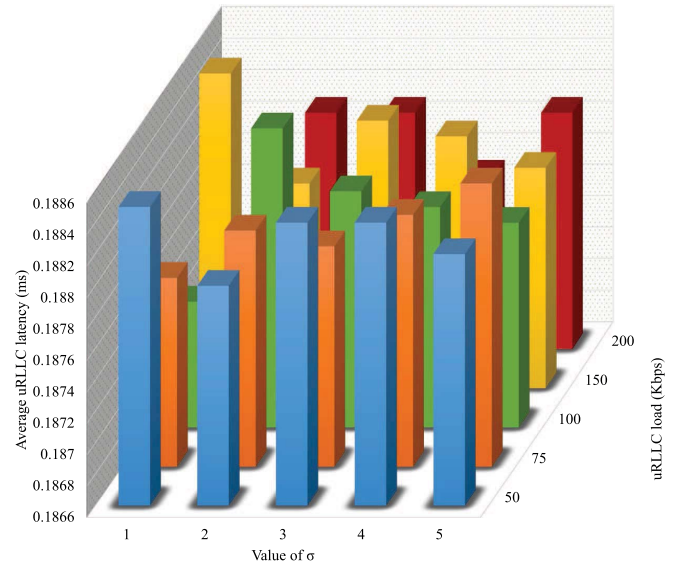
Fig. 9. Comparison of fairness score with varying value of σ and $L = 32$ Bytes.

the case of average *MEAR*. The figure also explicates that the average *MEAR* is declining with the growing value of σ due to the additional requirement of PRBs for extra *uRLLC* traffic. Particularly, our method results 10.20%, 10.87%, 5.77%, 5.77%, and 18.55% higher on average *MEAR* than those of RS, EDS, MBS, PS, and MUPS, respectively, for $\sigma = 1$. Moreover, similar values are 15.22%, 16.43%, 6.22%, 3.75%, and 70.20% for $\sigma = 10$. The average fairness score emerging from our method is bigger than or similar to other comparing methods for different values of σ and shown in Fig. 9. Fig. 9 also reveals that the σ value has a negligible impact on the average score of the fairness in the Proposed, RS, EDS, MBS, PS methods, but it impacts inversely to the MUPS method more and more *uRLLC* traffic choose same *eMBS* UE for the PRBs. Moreover, the average fairness scores of the proposed method are similar to both MBS and PS methods. However, the proposed method treats *eMBS* UEs 0.92%, 0.92%, and 1.92% fairly than RS, EDS, and MUPS methods, respectively,


 Fig. 10. Comparison of average *MEAR* with varying *uRLLC* load and σ .

 Fig. 11. Comparison of average fairness score with varying *uRLLC* load and σ .

when $\sigma = 1$, whereas, the similar scores are 1.23%, 1.23%, and 12.21%, respectively, during $\sigma = 10$.

In Fig. 10, we compare the average *MEAR* of *eMBB* UEs for considering varying *uRLLC* load (L) and *uRLLC* traffic (σ). The *MEAR* value of our method surpasses other concerned methods in every circumstance as revealed from Fig. 10. The same figure also explicates that these values degrade when L increases for varying σ as the system needs to allocate more PRBs to the *uRLLC* UEs. Moreover, these values decrease with the increasing value of σ for a fixed L , and also the same for increasing the value of L with a fixed σ . In Fig. 11, we compare the average fairness score of *eMBB* UEs for the different methods for changing the *uRLLC* load (L) and *uRLLC* traffic (σ). Fig. 11 exposes that the fairness scores of our method are better than or at least similar to that of its' rivals. The figure also reveals that these scores decrease with an increasing L for the lower value of σ . However, these scores increase with the increasing L when σ value is high.


 Fig. 12. Comparison of average *uRLLC* latency with varying *uRLLC* load and σ .

Moreover, for the MUPS method, these values decrease with the increasing value of σ and L .

In Fig. 12, we compare the average latency for *uRLLC* traffic with varying value of σ and *uRLLC* load (L). The Fig. 12 reveals that the average *uRLLC* latency is below 0.25 ms, which is the requirement for *uRLLC* traffic, for all considered cases. Moreover, this average *uRLLC* latency has no relation with the value of σ and L as all of the *uRLLC* traffics are served in one mini-slot for all the considered scenarios. However, the small differences of average latency values are due to the arrival period of *uRLLC* traffics within a mini-slot.

VI. CONCLUSION

In this paper, we have introduced a novel approach for coexisting *uRLLC* and *eMBB* traffic in the same radio resource for enabling 5G wireless systems. We have expressed the coexisting dilemma as a maximizing problem of the *MEAR* value of *eMBB* UEs meanwhile attending the *uRLLC* traffic. We handle the problem with the help of the decomposition strategy. In every time slot, we resolve the resource scheduling sub-problem of *eMBB* UEs using a *PSUM* based algorithm, whereas the similar sub-problem of *uRLLC* UEs is unraveled through optimal transportation model, namely *MCC* and *MODI* methods. For the efficient scheduling of PRBs among *eMBB* UEs, we also present a heuristic algorithm. Our extensive simulation outcomes demonstrate a notable performance gain of the proposed approach over the baseline approaches in the considered indicators.

APPENDIX

GENERALIZATION OF THE PROPOSED MODEL INTO MULTICELL MODEL

Considering multiple gNBs onto our system model would result in an interference. Considering multiple gNBs onto our system model would result in an interference component on the SINR expression, and this will help us to generalize

the model. This is because multiple gNBs consider physical resource reuse, where frequencies are reused at spatially separated locations to increase spectral efficiency. To achieve that, the SNR term will be replaced by SINR. Let $\mathcal{G} = \{1, \dots, G\}$ be the set of gNBs; thus, the SINR can be calculated as follows:

$$\gamma_{e,k}^{t,g} = \frac{P_e h_e^2}{I'_g + N_0 B}, \quad \forall g \in \mathcal{G}, g' \neq g, \quad (37)$$

where I'_g represents the corresponding interference at gNB $g \in \mathcal{G}$ from all other gNBs $g' \in \mathcal{G}$.

REFERENCES

- [1] *Cisco Visual Networking Index: Global Mobile Data Traffic Forecast Update, 2016–2021*, Cisco, San Jose, CA, USA, Jun. 2017.
- [2] *5G Service Roadmap 2022*, 5G Forum, Bangalore, India, Mar. 2016.
- [3] *IMT Vision-Framework and Overall Objectives of the Future Development of IMT for 2020 and Beyond*, document ITU-R M.2083-0, Sep. 2015.
- [4] *3GPP TSG RAN WGI Meeting #87*, document R1-1612306, 3GPP, Nov. 2016.
- [5] *Downlink Multiplexing of eMBB and URLLC Transmission*, document R1-1700374, 3GPP, Jan. 2017.
- [6] A. K. Bairagi, S. F. Abedin, N. H. Tran, D. Niyato, and C. S. Hong, "QoE-enabled unlicensed spectrum sharing in 5G: A game-theoretic approach," *IEEE Access*, vol. 6, pp. 50538–50554, Sep. 2018.
- [7] A. K. Bairagi, N. H. Tran, W. Saad, and C. S. Hong, "Bargaining game for effective coexistence between LTE-U and Wi-Fi systems," in *Proc. NOMS-IEEE/IFIP Netw. Oper. Manage. Symp.*, Apr. 2018, pp. 1–8.
- [8] S. Liu, F. Yang, J. Song, and Z. Han, "Block sparse Bayesian learning-based NB-IoT interference elimination in LTE-advanced systems," *IEEE Trans. Commun.*, vol. 65, no. 10, pp. 4559–4571, Oct. 2017.
- [9] S. F. Abedin, M. G. R. Alam, S. M. A. Kazmi, N. H. Tran, D. Niyato, and C. S. Hong, "Resource allocation for ultra-reliable and enhanced mobile broadband IoT applications in fog network," *IEEE Trans. Commun.*, vol. 67, no. 1, pp. 489–502, Jan. 2019.
- [10] R. Kassab, O. Simeone, and P. Popovski, "Coexistence of URLLC and eMBB services in the C-RAN uplink: An information-theoretic study," in *Proc. IEEE Global Commun. Conf. (GLOBECOM)*, Dec. 2018, pp. 1–6.
- [11] K. Ying, J. M. Kowalski, T. Nogami, Z. Yin, and J. Sheng, "Coexistence of enhanced mobile broadband communications and ultra-reliable low-latency communications in mobile front-haul," *Proc. SPIE*, vol. 10559, Jan. 2018, Art. no. 105590C.
- [12] G. Pocovi, K. I. Pedersen, and P. Mogensen, "Joint link adaptation and scheduling for 5G ultra-reliable low-latency communications," *IEEE Access*, vol. 6, pp. 28912–28922, May 2018.
- [13] P. Popovski, K. F. Trillingsgaard, O. Simeone, and G. Durisi, "5G wireless network slicing for eMBB, URLLC, and mMTC: A communication-theoretic view," *IEEE Access*, vol. 6, pp. 55765–55779, Sep. 2018.
- [14] H. Ji, S. Park, J. Yeo, Y. Kim, J. Lee, and B. Shim, "Ultra-reliable and low-latency communications in 5G downlink: Physical layer aspects," *IEEE Wirel. Commun.*, vol. 25, no. 3, pp. 124–130, Jun. 2018.
- [15] M. Bennis, M. Debbah, and H. V. Poor, "Ultra-reliable and low-latency wireless communication: Tail, risk and scale," *Proc. IEEE*, vol. 106, no. 10, pp. 1834–1853, 2018.
- [16] Q. Liao, P. Baracca, D. Lopez-Perez, and L. G. Giordano, "Resource scheduling for mixed traffic types with scalable TTI in dynamic TDD systems," in *Proc. IEEE Globecom Workshops (GC Wkshps)*, Dec. 2016, pp. 1–7.
- [17] K. I. Pedersen, G. Berardinelli, F. Frederiksen, P. Mogensen, and A. Szufarska, "A flexible 5G frame structure design for frequency-division duplex cases," *IEEE Commun. Mag.*, vol. 54, no. 3, pp. 53–59, Mar. 2016.
- [18] K. Pedersen, G. Pocovi, J. Steiner, and A. Maeder, "Agile 5G scheduler for improved E2E performance and flexibility for different network implementations," *IEEE Commun. Mag.*, vol. 56, no. 3, pp. 210–217, Mar. 2018.
- [19] C.-P. Li, J. Jiang, W. Chen, T. Ji, and J. Smee, "5G ultra-reliable and low-latency systems design," in *Proc. Eur. Conf. Netw. Commun. (EuCNC)*, Jun. 2017, pp. 1–5.
- [20] Z. Wu, F. Zhao, and X. Liu, "Signal space diversity aided dynamic multiplexing for eMBB and URLLC traffics," in *Proc. 3rd IEEE Int. Conf. Comput. Commun. (ICCC)*, Dec. 2017, pp. 1396–1400.
- [21] K. I. Pedersen, G. Pocovi, J. Steiner, and S. R. Khosravirad, "Punctured scheduling for critical low latency data on a shared channel with mobile broadband," in *Proc. IEEE 86th Veh. Technol. Conf. (VTC-Fall)*, Sep. 2017, pp. 1–6.
- [22] A. K. Bairagi, M. S. Munir, S. F. Abedin, and C. S. Hong, "Coexistence of eMBB and uRLLC in 5G wireless networks," in *Proc. Korea Comp. Cong.*, Jun. 2018, pp. 1377–1379.
- [23] A. K. Bairagi, M. S. Munir, M. Alsenwi, N. H. Tran, and C. S. Hong, "A matching based coexistence mechanism between eMBB and uRLLC in 5G wireless networks," in *Proc. 34th ACM/SIGAPP Symp. Appl. Comput.*, Apr. 2019, pp. 2377–2384.
- [24] K. I. Pedersen, G. Pocovi, and J. Steiner, "Preemptive scheduling of latency critical traffic and its impact on mobile broadband performance," in *Proc. IEEE 87th Veh. Technol. Conf. (VTC)*, Jun. 2018, pp. 1–6.
- [25] A. A. Esswie and K. I. Pedersen, "Multi-user preemptive scheduling for critical low latency communications in 5G networks," in *Proc. IEEE Symp. Comput. Commun. (ISCC)*, Jun. 2018, pp. 136–141.
- [26] A. A. Esswie and K. I. Pedersen, "Opportunistic spatial preemptive scheduling for URLLC and eMBB coexistence in multi-user 5G networks," *IEEE Access*, vol. 6, pp. 38451–38463, Jul. 2018.
- [27] A. Anand, G. de Veciana, and S. Shakkottai, "Joint scheduling of URLLC and eMBB traffic in 5G wireless networks," *IEEE/ACM Trans. Netw.*, vol. 28, no. 2, pp. 477–490, Apr. 2020.
- [28] R. Kassab, O. Simeone, P. Popovski, and T. Islam, "Non-orthogonal multiplexing of ultra-reliable and broadband services in fog-radio architectures," *IEEE Access*, vol. 7, pp. 13035–13049, Jan. 2019.
- [29] M. Alsenwi, N. H. Tran, M. Bennis, A. Kumar Bairagi, and C. S. Hong, "EMBB-URLLC resource slicing: A risk-sensitive approach," *IEEE Commun. Lett.*, vol. 23, no. 4, pp. 740–743, Apr. 2019.
- [30] *Study on New Radio Access Technology Physical Layer Aspects*, document 3GPP RT 38.802v14.0.0, 3GPP, Mar. 2017.
- [31] J. Zhang and J. G. Andrews, "Adaptive spatial intercell interference cancellation in multicell wireless networks," *IEEE J. Sel. Areas Commun.*, vol. 28, no. 9, pp. 1455–1468, Dec. 2010.
- [32] J. Scarlett, V. Y. F. Tan, and G. Durisi, "The dispersion of nearest-neighbor decoding for additive non-Gaussian channels," *IEEE Trans. Inf. Theory*, vol. 63, no. 1, pp. 81–92, Jan. 2017.
- [33] N. Zhang, Y.-F. Liu, H. Farmanbar, T.-H. Chang, M. Hong, and Z.-Q. Luo, "Network slicing for service-oriented networks under resource constraints," *IEEE J. Sel. Areas Commun.*, vol. 35, no. 11, pp. 2512–2521, Nov. 2017.
- [34] P. Liu, Y.-F. Liu, and J. Li, "An iterative reweighted minimization framework for joint channel and power allocation in the OFDMA system," in *Proc. IEEE Int. Conf. Acoust., Speech Signal Process. (ICASSP)*, Apr. 2015, pp. 3068–3072.
- [35] D. R. Hunter and K. Lange, "A tutorial on MM algorithms," *Amer. Statistician*, vol. 58, no. 1, pp. 30–37, Feb. 2004.
- [36] M. Razaviyayn, M. Hong, and Z.-Q. Luo, "A unified convergence analysis of block successive minimization methods for non-smooth optimization," *SIAM J. Optim.*, vol. 23, no. 2, pp. 1126–1153, Jan. 2013.
- [37] F. L. Hitchcock, "The distribution of a product from several sources to numerous localities," *J. Math. Phys.*, vol. 20, nos. 1–4, pp. 224–230, Apr. 1941.
- [38] G. B. Dantzig, *Linear Programming and Extensions*. Princeton, NJ, USA: Princeton Univ. Press, 1963.
- [39] N. V. Reinfield and W. R. Vogel, *Mathematical Programming*. Englewood Cliffs, NJ, USA: Prentice-Hall, 1958.
- [40] D. Shimshak, J. Alan Kaslik, and T. Barclay, "A modification of Vogel's approximation method through the use of heuristics," *Inf. Syst. Oper. Res.*, vol. 19, no. 3, pp. 259–263, Aug. 1981.
- [41] A. Charnes and W. W. Cooper, "The stepping stone method of explaining linear programming calculations in transportation problems," *Manag. Sci.*, vol. 1, no. 1, pp. 49–69, Oct. 1954.
- [42] H. A. Taha, *Operations Research: An Introduction*. Upper Saddle River, NJ, USA: Pearson, 2007.
- [43] R. Jain, D. M. Chiu, and W. R. Hawe, "A quantitative measure of fairness and discrimination for resource allocation in shared computer system," Eastern Res. Lab., Digit. Equip. Corp., Maynard, MA, USA, Tech. Rep. TR 301, Sep. 1984, vol. 38.
- [44] D. Julian, "Erasure networks," in *Proc. IEEE Int. Symp. Inf. Theory*, Jun. 2003, p. 138.
- [45] Y. Huang, S. Li, C. Li, Y. T. Hou, and W. Lou, "A deep-reinforcement-learning-based approach to dynamic eMBB/URLLC multiplexing in 5G NR," *IEEE Internet Things J.*, vol. 7, no. 7, pp. 6439–6456, Jul. 2020, doi: 10.1109/JIOT.2020.2978692.



Anupam Kumar Bairagi (Member, IEEE) received the B.Sc. and M.Sc. degrees in computer science and engineering from Khulna University (KU), Bangladesh, and the Ph.D. degree in computer engineering from Kyung Hee University, South Korea. He is currently an Associate Professor with the Discipline of Computer Science and Engineering, Khulna University. He has authored and coauthored around 40 publications, including refereed IEEE/ACM journals and conference papers. He has served as a Technical Program Committee member for different international conferences. His research interests include wireless resource management in 5G and beyond, healthcare, IIoT, cooperative communication, and game theory.



for different international conferences. His research interests include wireless resource management in 5G and beyond, healthcare, IIoT, cooperative communication, and game theory.

Md. Shirajum Munir (Graduate Student Member, IEEE) received the B.S. degree in computer science and engineering from Khulna University, Khulna, Bangladesh, in 2010. He is currently pursuing the Ph.D. degree in computer science and engineering with Kyung Hee University, Seoul, South Korea. He has served as a Lead Engineer for the Solution Laboratory, Samsung Research and Development Institute, Dhaka, Bangladesh, from 2010 to 2016. His current research interests include IoT network management, fog computing, mobile edge computing, software-defined networking, smart grid, and machine learning.



under several research projects funded by the Egyptian Government. His research interests include wireless communications and networking, resource slicing in 5G wireless networks, ultra reliable low latency communications (URLLC), UAV-assisted wireless networks, and machine learning.

Madyan Alsenwi received the B.E. and M.Sc. degrees in electronics and communications engineering from Cairo University, Egypt, in 2011 and 2016, respectively. He is currently pursuing the Ph.D. degree in computer science and engineering with Kyung Hee University, South Korea. He is also working as a Leading Researcher with the Intelligent Networking Laboratory under a project jointly funded by the prestigious Brain Korea 21st Century Plus and Ministry of Science and ICT, South Korea. Prior to this, he worked as a Research Assistant



include distributed computing and learning over networks. He received the Best KHU Thesis Award in engineering in 2011, and several best paper awards, including the IEEE ICC 2016, APNOMS 2016, and IEEE ICCS 2016. He receives the Korea NRF Funding for Basic Science and Research from 2016 to 2023. He has been an Editor of IEEE TRANSACTIONS ON GREEN COMMUNICATIONS AND NETWORKING since 2016.

Nguyen H. Tran (Senior Member, IEEE) received the B.S. degree in electrical and computer engineering from the Hochiminh City University of Technology in 2005 and the Ph.D. degree in electrical and computer engineering from Kyung Hee University in 2011. He was an Assistant Professor with the Department of Computer Science and Engineering, Kyung Hee University, from 2012 to 2017. Since 2018, he has been with the School of Computer Science, The University of Sydney, where he is currently a Senior Lecturer. His research interests



include distributed computing and learning over networks. He received the Best KHU Thesis Award in engineering in 2011, and several best paper awards, including the IEEE ICC 2016, APNOMS 2016, and IEEE ICCS 2016. He receives the Korea NRF Funding for Basic Science and Research from 2016 to 2023. He has been an Editor of IEEE TRANSACTIONS ON GREEN COMMUNICATIONS AND NETWORKING since 2016.



Mehedi Masud (Senior Member, IEEE) received the Ph.D. degree in computer science from the University of Ottawa, Canada. He is currently a Professor with the Department of Computer Science, Taif University, Taif, Saudi Arabia. He has authored and coauthored around 70 publications, including refereed IEEE/ACM/Springer/Elsevier journals, conference papers, books, and book chapters. He has served as a Technical Program Committee member for different international conferences. His research interests include machine learning, distributed algorithms, data security, formal methods, and health analytics. He was a recipient of a number of awards, including the Research in Excellence Award from Taif University. He is on the Associate Editorial Board of IEEE ACCESS, *International Journal of Knowledge Society Research* (IJKSR), and an Editorial Board member of *Journal of Software*. He has also served as a Guest Editor for *Computer Science and Information Systems* (ComSIS) Journal and *Journal of Universal Computer Science* (JUCS). He is also a member of ACM.



Zhu Han (Fellow, IEEE) received the B.S. degree in electronic engineering from Tsinghua University, in 1997, and the M.S. and Ph.D. degrees in electrical and computer engineering from the University of Maryland, College Park, in 1999 and 2003, respectively. From 2000 to 2002, he was a Research and Development Engineer with JDSU, Germantown, MD, USA. From 2003 to 2006, he was a Research Associate with the University of Maryland. From 2006 to 2008, he was an Assistant Professor with Boise State University, Idaho. He is currently a John and Rebecca Moores Professor with the Department of Electrical and Computer Engineering, and the Department of Computer Science, University of Houston, Houston, TX, USA. His research interests include wireless resource allocation and management, wireless communications and networking, game theory, big data analysis, security, and smart grid. He received an NSF Career Award in 2010, the Fred W. Ellersick Prize of the IEEE Communication Society in 2011, the EURASIP Best Paper Award for the Journal on Advances in Signal Processing in 2015, IEEE Leonard G. Abraham Prize in the field of Communications Systems [Best Paper Award in IEEE JOURNAL ON SELECTED AREAS IN COMMUNICATIONS (JSAC)] in 2016, and several best paper awards in IEEE conferences. He has been an IEEE Communications Society Distinguished Lecturer from 2015 to 2018, the AAAS Fellow since 2019, and the ACM distinguished Member since 2019. He has also been 1% highly cited researcher since 2017 according to Web of Science. He is also the winner of 2021 IEEE Kiyo Tomiyasu Award, for outstanding early to mid-career contributions to technologies holding the promise of innovative applications, with the following citation: “for contributions to game theory and distributed management of autonomous communication networks.”



Choong Seon Hong (Senior Member, IEEE) received the B.S. and M.S. degrees in electronic engineering from Kyung Hee University, Seoul, South Korea, in 1983 and 1985, respectively, and the Ph.D. degree from Keio University, Japan, in 1997. In 1988, he joined KT, where he was involved in broadband networks as a Member of Technical Staff. Since 1993, he has been with Keio University. He was with the Telecommunications Network Laboratory, KT, as a Senior Member of Technical Staff and as the Director of the Networking Research Team until 1999. Since 1999, he has also been a Professor with the Department of Computer Science and Engineering, Kyung Hee University. His research interests include future Internet, ad hoc networks, network management, and network security. He is also a member of ACM, the IEICE, the IPSJ, the KIISE, the KICS, the KIPS, and the OSIA. He has served as the General Chair, the TPC Chair/Member, or an Organizing Committee member for international conferences, such as NOMS, IM, APNOMS, E2EMON, CCNC, ADSN, ICPP, DIM, WISA, BcN, TINA, SAINT, and ICOIN. He was an Associate Editor of IEEE TRANSACTIONS ON NETWORK AND SERVICE MANAGEMENT and *IEEE Journal of Communications and Networks*. He currently serves as an Associate Editor for *International Journal of Network Management* and an Associate Technical Editor for *IEEE Communications Magazine*.